Self-biased magnetoelectric responses in magnetostrictive/piezoelectric composites with different high-permeability alloys*

Lu Cai-Jiang(鲁彩江), Li Ping(李 平)†, Wen Yu-Mei(文玉梅), Yang Ai-Chao(杨爱超), Yang Chao(杨 超), Wang De-Cai(王德才), He Wei(何 伟), and Zhang Ji-Tao(张吉涛)

Research Center of Sensors and Instruments, College of Optoelectronic Engineering, Chongqing University, Chongqing 400044, *China*

(Received 26 February 2014; revised manuscript received 14 May 2014; published online 21 October 2014)

We comparatively investigate the influence of various high-permeability alloys on the hysteretic and remanent resonant magnetoelectric (ME) response in a composite of magnetostrictive nickel (Ni) and piezoelectric $Pb(Zr_{1-x}, Ti_x)O_3$ (PZT). In order to implement this comparative research, Co-based amorphous alloy (CoSiB), Fe-based nanocrystalline alloy (FeCuNbSiB) and Fe-based amorphous alloy (FeSiB) are used according to different magnetostriction (λ_s) and saturation magnetization ($\mu_0 M_s$) characteristics. The bending and longitudinal resonant ME voltage coefficients ($\alpha_{ME,b}$ and $\alpha_{ME,l}$) are observed comparatively for CoSiB/Ni/PZT, FeCuNbSiB/Ni/PZT, and FeSiB/Ni/PZT composites. The experimental data indicate that the FeSiB/Ni/PZT composite has the largest remanent self-biased $\alpha_{ME,b}$ and $\alpha_{ME,l}$ due to the largest magnetic grading of λ_s and $\mu_0 M_s$ in the FeSiB/Ni layer. When the number of FeSiB foils is four, the maximum remanent $\alpha_{ME,b}$ and $\alpha_{ME,l}$ at zero bias magnetic field are 57.8 V/cm·Oe and 107.6 V/cm·Oe, respectively. It is recommended that the high-permeability alloy is supposed to have larger λ_s and $\mu_0 M_s$ for obtaining a larger remanent self-biased ME responses in ME composite with high-permeability alloy.

Keywords: magnetoelectric effect, composite materials, high-permeability alloy

PACS: 75.85.+t, 85.80.Jm, 77.84.Lf, 81.07.Bc **DOI:** 10.1088/1674-1056/23/11/117503

1. Introduction

The magnetoelectric (ME) effect, which exhibits an electric polarization response to an applied magnetic field or a magnetization response to an applied electric field, has been studied extensively because of the potential applications of devices, such as passive magnetic field sensors,[1] electric current sensors,[2–4] magnetoelectric transducers,[5] current-voltage converters,[6] etc. In the past few years, large resonant ME responses have been reported in composites of piezoelectric $Pb(Zr,Ti)O_3$ (PZT) or $Pb(Mg_{1/3}Nb_{2/3})O_3$ layers laminated with magnetostrictive Terfenol-D, FeNi, Ni, or metglas ones.[7–11] In order to enable potential applications, efforts for enhancing the ME responses have been made in various aspects.[11–13] Unfortunately, the ME composites require the presence of external dc bias magnetic field H_{dc} for achieving large ME responses.[1–13] In practical applications, the need of an H_{dc} presents some significant disadvantages. For example, the required space is increased and a potential noise source is added. Therefore, the self-biased ME composites are necessary and have been investigated in previous papers.[14–21]

Recently, the ME composite with exchange biasing effect has shown an ME response under zero magnetic bias field.[16] The magnetic exchange occurs only at the thin interface (∼nm in thickness), so this thin ME structure is difficult to fabricate and potentially costly compared to laminate composite. Besides, the use of a magnetization-graded magnetic layer is a feasible approach for achieving the self-biased ME responses in the case of laminate composite.[17–21] By attaching high-permeability (high-μ) alloys at the bottom of the magnetostrictive materials, the magnetization-graded magnetic layers are formed.[18–21] Various high-μ alloys differ widely in their magnetic characteristics, such as the magnetostriction (λ_s) and the saturation magnetization ($\mu_0 M_s$). Therefore, there are some discrepancies in the ME responses of composites with different high-μ alloys. However, up to now, few studies have focused on these discrepancies. Actually, for practical applications of the composites, it is both physically interesting and technologically important to systematically investigate the differences in the ME responses of the ME composites with different high-μ alloys.

In this paper, we comparatively investigate the resonant ME responses in bilayer composite Ni/PZT (NP) with different high-μ alloys. Samples of CoSiB/Ni/PZT, FeCuNbSiB/Ni/PZT, and FeSiB/Ni/PZT are used for measurements of ME voltage coefficients at bending and longitudinal resonant frequencies ($\alpha_{ME,b}$ and $\alpha_{ME,l}$, respectively). The experimental results demonstrate that the high-μ alloys should have larger λ_s and $\mu_0 M_s$ in order to obtain a larger self-biased ME re-

*Project supported by the National High Technology Research and Development Program of China (Grant No. 2012AA040602) and the National Natural Science Foundation of China (Grant No. 61374217).

†Corresponding author. E-mail: liping@cqu.edu.cn

© 2014 Chinese Physical Society and IOP Publishing Ltd

sponse. This comparative study provides the basic design of a self-biased ME composite with a high-μ alloy to obtain a larger ME response.

2. Experimental details

2.1. Structure and material characteristics

Figure 1(a) illustrates the schematic diagram of the ME composite Ni/PZT with high-μ alloys. The high-μ alloy foils are attached at the bottom of the Ni plate. The magnetostriction (λ_s) and saturation magnetization ($\mu_0 M_s$) are important characteristics for the high-μ alloys. Therefore, according to these material characteristics, three kinds of high-μ alloys are chosen to compare their influences on the ME effects of NP. The prototypes of materials are shown in Fig. 1(b) and the material characteristics are shown in Table 1. The negative magnetostrictive Ni has $\mu_r = 200$, $\lambda_s = 40$ ppm and $\mu_0 M_s = 0.616$ T. In order to compare the stress effect of high-μ alloys on NP composite, we chose Co-based amorphous alloy (CoSiB) without magnetostiction ($\lambda_{s-CoSiB} = 0$ ppm), Fe-based nanocrystalline alloy (FeCuNbSiB) with $\lambda_{s-FeCuNbSiB} = 2.7$ ppm and Fe-based amorphous alloy (FeSiB) with $\lambda_{s-FeSiB} = 27$ ppm. For comparing the influences of $\mu_0 M_s$, we chose CoSiB with low $\mu_0 M_s$ ($\mu_0 M_{s-CoSiB} = 0.53$ T$< \mu_0 M_{s-Ni} = 0.616$ T) and two alloys (FeCuNbSiB and FeSiB) which have larger $\mu_0 M_s$ than that of Ni ($\mu_0 M_{s-Ni} = 0.616$ T$< \mu_0 M_{s-FeCuNbSiB} = 1.25$ T$<$ $\mu_0 M_{sFeSiB} = 1.56$ T). The relationships for permeability μ_r is $\mu_{r-CoSiB} > \mu_{r-FeCuNbSiB} > \mu_{r-FeSiB} > \mu_{r-Ni}$.

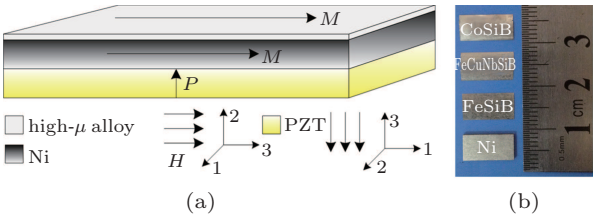


Fig. 1. (color online) (a) Schematic illustration of ME composite Ni/PZT with high-μ alloys. (b) Photographs of the magnetostrictive materials CoSiB, FeCuNbSiB, FeSiB, and Ni.

Table 1. Material characteristics of Ni, CoSiB, FeCuNbSiB, and FeSiB.

	Ni	Co-based amorphous alloy 2714A (CoSiB)	Fe-based nanocrystalline alloy 1K107 (FeCuNbSiB)	Fe-based amorphous alloy 2605-S2 (FeSiB)
μ_r	200	90000	$\geq$ 50000	30000
λ_s/ppm	−40	0	+2.7	+27
$\mu_0 M_s$/T	0.616	0.53	1.25	1.56
ρ/g·cm^{-3}	8.9	7.7	7.4	7.18

2.2. Measurement setup

The dimensions of the three kinds of high-μ alloys are $12 \times 6 \times 0.03$ mm^3 ($l \times w \times t$). The annealed, 99.6% pure Ni are cut to rectangular plates with $12 \times 6 \times 1$ mm^3 ($l \times w \times t$). The piezoelectric plates are PZT8 of $12 \times 6 \times 1$ mm^3 ($l \times w \times t$). Firstly, the Ni plates, PZT plates and high-μ alloy foils are dipped in an organic impregnant to clean them. Secondly, the samples of NP composites were fabricated by stacking and bonding with an insulated epoxy adhesive. Then the samples were kept at 80 °C for 1 h to cure the epoxy for good mechanical coupling. For samples with higher thickness of high-μ alloy foils, it is necessary to bond the required 30 μm-thick high-μ alloy foils with cyanoacrylate adhesive. The high-μ alloy foils with different thickness were then bonded to Ni with a 2-μm to 3-μm-thick layer of cyanoacrylate adhesive.

The strength of ME interaction is defined in terms of the ME voltage coefficient $\alpha_{ME} = dE/dH = dV/(t\,dH)$, where dV is the induced voltage, and t is the composite thickness. In experiments, the applied dc bias magnetic field (H_{dc}) was generated by a pair of neodymium permanent magnets (NbFeB), and an alternating current magnetic field (H_{ac}) was generated by a long-straight solenoid coil driven by a signal generator (Tektronix AFG3021B). Different values of $H_{dc} = 0$–600 Oe were realized by adjusting the distance of NbFeB magnets, and were measured by a Gauss meter. The middle supported ME samples were placed at the center of the long-straight solenoid coil. The magnitude of $H_{ac} = 0.2$ Oe was realized by using a virtual instrument (Labview VI program) to monitor the output signal of a signal generator (Tektronix AFG3021B). The output voltages across two silver electrodes of PZT were transferred to a filter (Stanford research systems SR560) and then were detected by a Labview VI program. As a result, the ME voltage coefficient α_{ME} can be obtained.

3. Results and discussion

Figure 2(a) shows the frequency dependence of the ME voltage coefficient α_{ME} for NP around bending-resonance frequency. The bias field H_{dc} is set to 274 Oe. From this figure, one can see that the bending-resonance frequency of NP is about 50.8 kHz. Figure 2(b) shows the frequency dependence of α_{ME} for NP around longitudinal-resonance frequency. The bias field H_{dc} is set to 320 Oe. One can see that the longitudinal-resonance frequency of NP is about

175.5 kHz. The longitudinal-resonance α_{ME} of 25.2 V/cm·Oe is far larger than the bending-resonance α_{ME} of 98 V/cm·Oe.

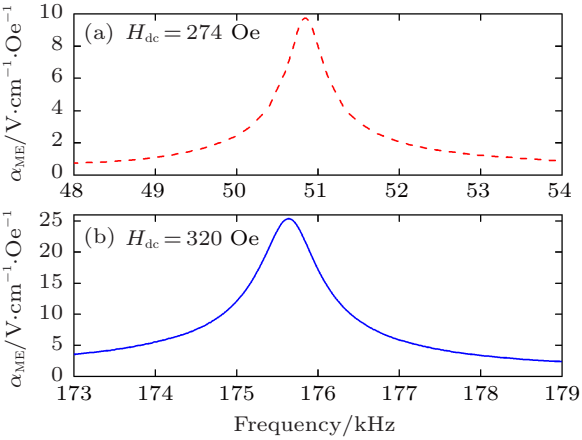


Fig. 2. (color online) Frequency dependence of the ME voltage coefficient α_{ME} for (a) NP around bending resonance and (b) NP around longitudinal resonance.

Then we measured the bending-resonance ME voltage coefficient ($\alpha_{ME,b}$) and longitudinal-resonance ME voltage coefficient ($\alpha_{ME,l}$) of NP at different H_{dc}. The H_{dc} dependences of $\alpha_{ME,b}$ and $\alpha_{ME,l}$ are shown in Figs. 3(a) and 3(b), respectively. In the up sweep, $\alpha_{ME,b}$ and $\alpha_{ME,l}$ of NP decrease first and then increase to a maximum value at optimum H_{dc}. Further increase in H_{dc} results in the decrease in the magnitudes of $\alpha_{ME,b}$ and $\alpha_{ME,l}$. According to this figure, the variation tendencies for $\alpha_{ME,b}$ and $\alpha_{ME,l}$ of NP in the down sweep are the same as those in the up sweep. $\alpha_{ME,b}$ and $\alpha_{ME,l}$ of NP in the down sweep are a little larger than those in the up sweep. These results demonstrate that NP composite has hysteresis behaviors, which can be attributed to the inherent hysteresis behavior in Ni.[15]

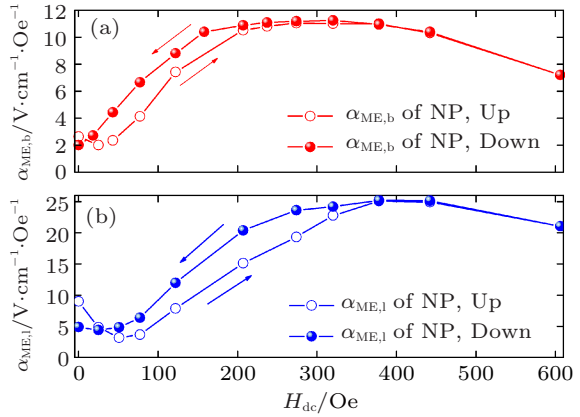


Fig. 3. (color online) (a) Bending-resonance ME voltage coefficient ($\alpha_{ME,b}$) of NP as a function of H_{dc}, and (b) the longitudinal-resonance ME voltage coefficient ($\alpha_{ME,l}$) of NP as a function of H_{dc}.

Figure 4(a) shows H_{dc} dependences of $\alpha_{ME,b}$ for NP and CoSiB/Ni/PZT (CS/NP) with one layer CoSiB ($L = 1$), and figure 4(b) shows H_{dc} dependences of $\alpha_{ME,l}$ for NP and CS/NP with $L = 1$. One can see clearly that both $\alpha_{ME,b}$ and $\alpha_{ME,l}$ increase only a little after incorporating one layer of CoSiB into the NP composite. The $\alpha_{ME,b}$ of CS/NP with $L = 1$ is 7.5 V·cm^{-1}·Oe^{-1} at optimal $H_{dc} = 274$ Oe, and $\alpha_{ME,l}$ of CS/NP with $L = 1$ is 24 V·cm^{-1}·Oe^{-1} at optimal $H_{dc} = 320$ Oe.

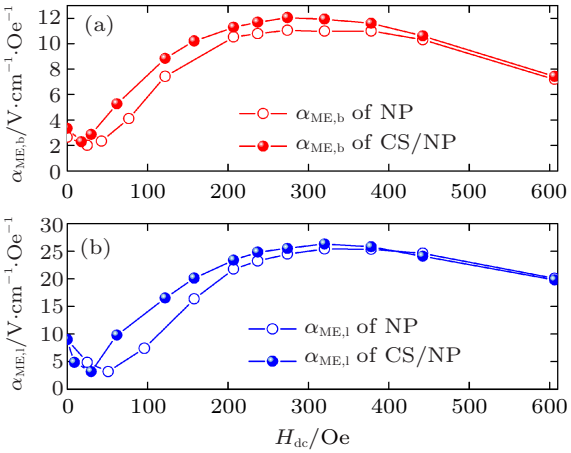


Fig. 4. (color online) (a) $\alpha_{ME,b}$ as a function of H_{dc} for NP, CS/NP with $L = 1$, and (b) $\alpha_{ME,l}$ as a function of H_{dc} for NP, CS/NP with $L = 1$.

Since the high-μ CoSiB has some influences on ME responses of NP, the influence of CoSiB thickness needs to be investigated in detail. The maximum $\alpha_{ME,b}$ ($\alpha_{ME,b-Max}$) of CS/NP and the needed optimum H_{dc} (H_{dc-op}) as a function of the CoSiB layers are shown in Fig. 5(a). The maximum $\alpha_{ME,l}$ ($\alpha_{ME,l-Max}$) of CS/NP and H_{dc-op} as a function of the CoSiB layers are shown in Fig. 5(b). The thickness of CoSiB varies from 0.03 mm to 0.15 mm (or the number of CoSiB layers $L = 1$–5). According to the data in this figure, $\alpha_{ME,b-Max}$ and $\alpha_{ME,l-Max}$ of CS/NP with one layer CoSiB are a little larger than those of NP. When $L > 1$, $\alpha_{ME,b-Max}$ and $\alpha_{ME,l-Max}$ of CS/NP decrease with increasing L, and are lower than those of NP. In comparison with NP, H_{dc-op} of CS/NP for $\alpha_{ME,b-Max}$ and $\alpha_{ME,l-Max}$ are nearly unchanged.

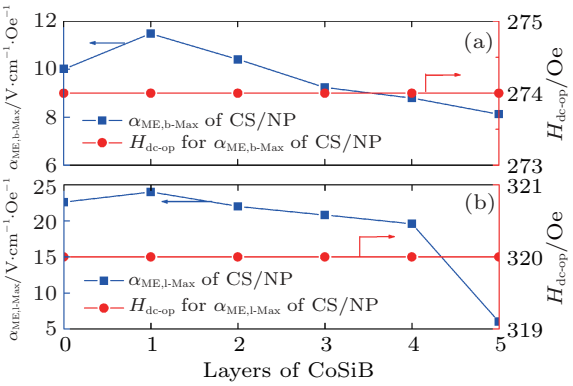


Fig. 5. (color online) (a) The maximum $\alpha_{ME,b}$ ($\alpha_{ME,b-Max}$) and the needed optimum H_{dc} (H_{dc-op}) for CS/NP as a function of the CoSiB layers. (b) The maximum $\alpha_{ME,l}$ ($\alpha_{ME,l-Max}$) and the needed optimum H_{dc} (H_{dc-op}) for CS/NP as a function of the CoSiB layers.

When the composite plates are subjected to a zero bias magnetic field and an AC magnetic field, the magnetic mo-

ments in high-μ ribbons rotate first due to its superior soft magnetostrictive characteristics. The Ni plate with a residual magnetization provides an additional bias magnetic field to high-μ ribbons. In addition, the high-μ ribbons drive the magnetic moments of Ni to rotate faster (or concentrate more magnetic flux in Ni). As a result, an internal magnetic field is generated between high-μ ribbon and Ni, which results in the enhanced self-biased ME effects. However, because the magnetostriction of high-μ CoSiB is zero, the rotations of magnetic moments in Ni are affected weakly by CoSiB. In addition, although the CoSiB has characteristics of high-μ, the saturation magnetization is lower than Ni ($\mu_0 M_{s-CoSiB} = 0.53$ T$< \mu_0 M_{s-Ni} = 0.616$ T). Consequently, the self-biased ME response of CS/NP is weak and the H_{dc-op} almost does not change with the increase of the layers of CoSiB ribbon (L). From these results, although CoSiB has high permeability, it cannot be used to obtain self-biased ME effects of NP due to its zero magnetostriction and lower $\mu_0 M_s$ than Ni.

In order to obtain the samples of FeCuNbSiB/Ni/PZT (FC/NP) and FeSiB/Ni/PZT (FS/NP), we added a layer of 0.03–0.15-mm-thick FeCuNbSiB and FeSiB (or the number of layers $L = 1$–5) to NP, respectively. Firstly, we measure $\alpha_{ME,b}$ of FC/NP and FS/NP. The H_{dc} dependence of $\alpha_{ME,b}$ for FC/NP with FeCuNbSiB layers $L = 1$–5 and FS/NP with FeSiB layers $L = 1$–5 are shown in Figs. 6(a) and 6(b), respectively. In Fig. 6, the phase information (an additional phase difference of 180° in ME output voltage) is considered. One can see clearly that (i) $\alpha_{ME,b}$ vs H_{dc} loops for FC/NP and FS/NP with $L = 1$–5 are clockwise with negative remanent $\alpha_{ME,b}$ and positive coercive fields, (ii) the loops move along the H_{dc} axis with increasing L, and (iii) the largest $\alpha_{ME,b}$ is achieved when $L = 4$. The inset of Fig. 6(a) shows the remanent zero-biased $\alpha_{ME,b}$ of FC/NP as a function of L. One observes that the largest zero-biased $\alpha_{ME,b}$ of FC/NP is 41.3 V/cm·Oe when $L = 4$. The data in Fig. 6(a) show a negative peak $\alpha_{ME,b}$ of 48.5 V/cm·Oe at $H_{dc} = 35$ Oe and a positive peak $\alpha_{ME,b}$ of 33.2 V/cm·Oe at $H_{dc} = 158$ Oe for FC/NP with $L = 4$. The remanent zero-biased $\alpha_{ME,b}$ of FS/NP as a function of L are shown in the inset of Fig. 6(b). When $L = 4$, one can observe clearly that the largest negative peak $\alpha_{ME,b}$ of −57.8 V/cm·Oe exactly appears at $H_{dc} = 0$ Oe, and the positive peak $\alpha_{ME,b}$ of 37.8 V/cm·Oe appears at $H_{dc} = 180$ Oe.

Finally, we measured $\alpha_{ME,l}$ of FC/NP and FS/NP composites. Figure 7(a) shows $\alpha_{ME,l}$–H_{dc} curves for FC/NP with $L = 1$–5. The phase information (an additional phase difference of 180° in ME output voltage) is also considered. It can be seen that $\alpha_{ME,l}$–H_{dc} loops of FC/NP are clockwise with negative remanent $\alpha_{ME,l}$ and positive coercive fields. With increasing L, the loops move along the H_{dc} axis. The $\alpha_{ME,l}$ increases until $L = 4$ and then decreases. The inset of Fig. 7(a) shows the remanent zero-biased $\alpha_{ME,l}$ of FC/NP as a function of L. The largest zero-biased $\alpha_{ME,l}$ for FC/NP with $L = 4$ is 89.7 V/cm·Oe. The negative peak $\alpha_{ME,l}$ of −90.5 V/cm·Oe for FC/NP with $L = 4$ appears at $H_{dc} = 30$ Oe. The positive peak $\alpha_{ME,l}$ for FC/NP with $L = 4$ at $H_{dc} = 158$ Oe is the largest of 60 V/cm·Oe. Figure 7(b) shows $\alpha_{ME,l}$–H_{dc} curves for FS/NP with $L = 1$–5. Compared with the $\alpha_{ME,l}$–H_{dc} curves of FC/NP, the $\alpha_{ME,l}$–H_{dc} curves of FS/NP are also clockwise with negative remanent $\alpha_{ME,l}$ and positive coercive fields. With increasing L, the loops move along the H_{dc} axis. When $L = 4$, the maximum zero-biased $\alpha_{ME,l}$ for FS/NP is 107.6 V/cm·Oe, the negative peak $\alpha_{ME,l}$ for FS/NP is −111.7 V/cm·Oe at $H_{dc} = -4$ Oe and the positive peak $\alpha_{ME,l}$ for FS/NP is 62.2 V/cm·Oe at $H_{dc} = 180$ Oe.

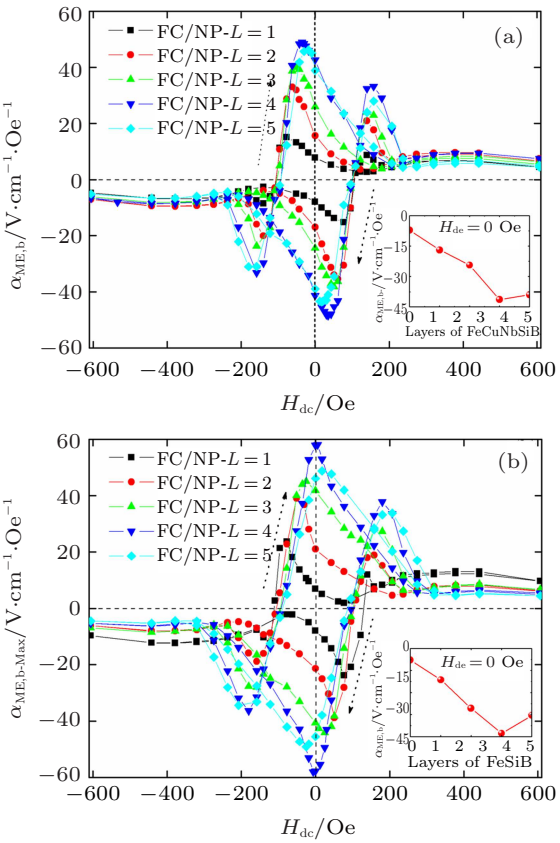


Fig. 6. (color online) The H_{dc} dependence of $\alpha_{ME,b}$ for (a) FC/NP and (b) FS/NP. The insets show $\alpha_{ME,b}$ for FC/NP and FS/NP at $H_{dc} = 0$ Oe as a function of L. The layers of FeCuNbSiB and FeSiB $L = 1$–5.

Comparing the data in Fig. 6(a) with that in Fig. 6(b) and the data in Fig. 7(a) with that in Fig. 7(b), respectively, we find that the FS/NP has larger $\alpha_{ME,b}$ and $\alpha_{ME,l}$ than FC/NP. As H_{dc} increases from 0 to 600 Oe, the magnitude of $\alpha_{ME,b}$ (or $\alpha_{ME,l}$) increases to a negative peak at optimal H_{dc} and then decrease to zero at a particular H_{dc}. Because the magnetic moments in FeCuNbSiB (or FeSiB) ribbons rotate first for its superior soft magnetostrictive characteristics, the negative peak is attributed to the magnetostriction of the FeCuNbSiB ribbon. Beyond the zero-crossing, there are two positive peak values of the $\alpha_{ME,b}$ (or $\alpha_{ME,l}$) with increasing H_{dc}. We can attribute the first peak

to the magnetostriction of Ni with flux concentration effect (the FeCuNbSiB ribbons concentrate more magnetic flux in Ni). As H_{dc} increases to about 442 Oe, the other positive peak of $\alpha_{ME,b}$ (or $\alpha_{ME,l}$) appears, which is attributed to the magnetostriction of Ni without flux concentration effect.

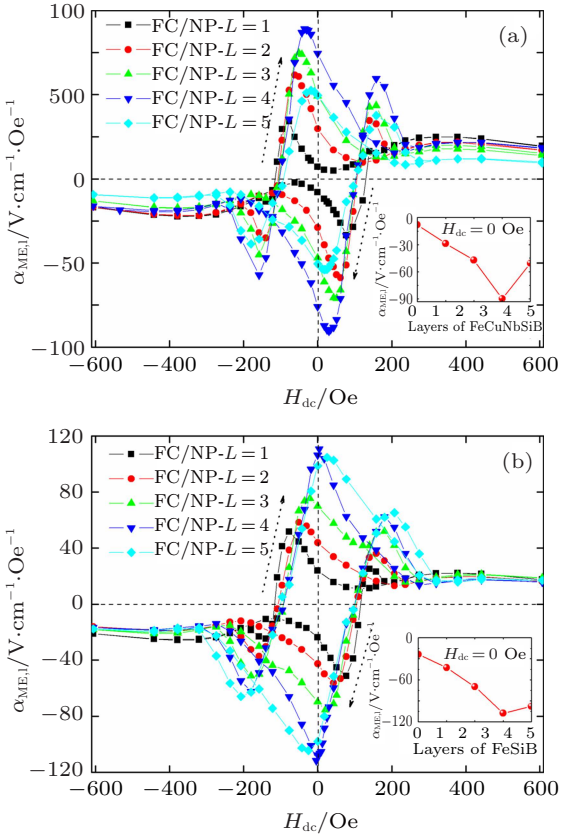


Fig. 7. (color online) The $\alpha_{ME,l}$ as a function of H_{dc} for NP samples with (a) FeCuNbSiB layers $L=1$–5, and (b) FeSiB layers $L=1$–5. The insets show $\alpha_{ME,l}$ for FC/NP and FS/NP at $H_{dc}=0$ Oe as a function of L.

As a result, the strong hysteresis behaviors of FC/NP (or FS/NP) can be attributed to the comprehensive coupling effect of FeCuNbSiB (or FeSiB) and Ni, such as internal magnetic field in FeCuNbSiB/Ni (or FeSiB/Ni) layer resulting from the magnetic coupling, the stress coupling of FeCuNbSiB (or FeSiB) and Ni. According to the material characteristics in Table 1, FeSiB has larger λ_s ($\lambda_{s-FeSiB}=27$ ppm$>$ $\lambda_{s-FeCuNbSiB}=27$ ppm) and $\mu_0 M_s$ ($\mu_0 M_{sFeSiB}=1.56$ T$>$ $\mu_0 M_{sFeCuNbSiB}=1.25$ T). Thus, the grading of λ_s and $\mu_0 M_s$ in FeSiB/Ni is larger than that in FeCuNbSiB/Ni. Since the grading results in the self-biased ME response, FS/NP should have larger $\alpha_{ME,b}$ and $\alpha_{ME,l}$ than those of FC/NP.

4. Conclusion

Comparative studies on bending and longitudinal resonant ME responses have been performed on CS/NP, FC/NP, and FS/NP composites. In CS/NP, the experimental data do not show self-biased ME responses for the zero-magnetostriction and low $\mu_0 M_s$ ($\mu_0 M_{s-CoSiB}=0.53$ T$<$ $\mu_0 M_{s-Ni}=0.616$ T) characteristics of CoSiB. Upon the grading of λ_s and $\mu_0 M_s$ in magnetostrictive layers FeCuNbSiB/Ni or FeSiB/Ni, an internal magnetic field is formed and results in a large self-biased ME response in FC/NP or FS/NP composite. In addition, the FS/NP composite with optimal layers of FeSiB has larger self-biased ME responses than those of FC/NP. This can be attributed to the larger grading of λ_s and $\mu_0 M_s$ in FeSiB/Ni than that in FeCuNbSiB/Ni. When $L=4$, the observed largest zero-biased $\alpha_{ME,b}$ and $\alpha_{ME,l}$ for FS/NP are 57.8 V/cm·Oe and 107.6 V/cm·Oe, respectively. It is recommended that the high-μ alloy should have larger λ_s and $\mu_0 M_s$ in order to obtain larger self-biased ME responses for NP with high-μ alloy.

References

[1] Zhai J Y, Dong S X, Xing Z P, Li J F and Viehland D 2007 *Appl. Phys. Lett.* **91** 123513

[2] Dong S X, Bai J G, Zhai J Y, Li J F, Lu G Q, Viehland D, Zhang S J and Shrout T R 2005 *Appl. Phys. Lett.* **86** 182506

[3] Zhang S Y, Leung C M, Kuang W and Ho S L 2013 *J. Appl. Phys.* **113** 17C733

[4] Zhang J T, Li P, Wen Y M, He W, Yang A C, Lu C J, Qiu J, Wen J, Yang J, Zhu Y and Yu M 2012 *Rev. Sci. Instrum.* **83** 115001

[5] Dai X Z, Wen Y M, Li P, Yang J and Li M 2011 *Sens. Actuat. A* **166** 94

[6] Jia Y M, Or S W, Chan H L W, Jiao J, Luo H S and van der Zwaag S 2009 *Appl. Phys. Lett.* **94** 263504

[7] Nan C W, Bichurin M I, Dong S X, Viehland D and Srinivasan G 2008 *J. Appl. Phys.* **103** 031101

[8] Yu G L, Li Y X, Zeng Y Q, Li J, Zuo L, Li Q and Zhang H W 2013 *Chin. Phys. B* **22** 077504

[9] Bi K, Wu W and Wang Y G 2011 *Chin. Phys. B* **20** 067503

[10] Chen L, Li P, Wen Y M and Wang D 2011 *Acta Phys. Sin.* **60** 067501 (in Chinese)

[11] Ma J, Hu J M, Li Z and Nan C W 2011 *Adv. Mater.* **23** 1062

[12] Li P, Wen Y M and Bian L X 2007 *Appl. Phys. Lett.* **90** 022503

[13] Lu C J, Li P, Wen Y M, Yang A C, He W and Zhang J T 2013 *Appl. Phys. Lett.* **102** 132410

[14] Mandal S K, Sreenivasulu G, Petrov V M and Srinivasan G 2010 *Appl. Phys. Lett.* **96** 192502

[15] Zhou Y, Yang S C, Apo D J, Maurya D and Priya S 2012 *Appl. Phys. Lett.* **101** 232905

[16] Lage E, Kirchhof C, Hrkac V, Kienle L, Jahns R, Knöche R, Quandt E and Meyners D 2012 *Nat. Mater.* **11** 523

[17] Yang S C, Park C S, Cho K H and Priya S 2010 *J. Appl. Phys.* **108** 093706

[18] Park C S, Cho K H, Arat M A, Evey J and Priya S 2010 *J. Appl. Phys.* **107** 094109

[19] Chen L, Li P, Wen Y M and Wang P 2012 *J. Appl. Phys.* **112** 024504

[20] Lu C J, Li P, Wen Y M, Yang A C, He W, Zhang J T, Yang J, Wen J, Zhu Y and Yu M 2013 *Appl. Phys. A* **113** 413

[21] Lu C J, Li P, Wen Y M, Yang A C, Yang C, Wang D C, He W and Zhang J T 2014 *J. Alloy. Compd.* **589** 498